

Nonlinear Spectroscopy

Richard G. Brewer

Frequently in physics the analysis of a problem is simplified by the use of a linear model. For example, the electrical current in a resistor depends linearly on the applied voltage, the displacement or strain of a rubber band is proportional to the stress, and, in spectroscopy, the amount of radiation absorbed by a molecular sample varies linearly with the intensity. As the voltage, stress, or intensity increases, however, the response may become nonlinear and the analysis more complex. Nonlinear spectroscopy, made possible by the availability of intense laser light, is an exception. Here, not only does the theory remain tractable, but the experimental techniques are elegantly simple and may have far-reaching consequences for such diverse subjects as molecular structure, the speed of light, the primary standard of length, transient coherence phenomena, and geophysics.

Nonlinear effects are known, of course, in other branches of spectroscopy: microwave spectroscopy (1), molecular beam resonance (2), nuclear magnetic resonance (3), and optical pumping (4). Nonetheless, with the exception of optical pumping, the nonlinear aspects are somewhat incidental to the main theme of these subjects. In this article I review a number of atomic and molecular nonlinear optical interactions which have evolved with lasers and now permit spectroscopic measurements of unprecedented precision. The nonlinear behavior, which is essential here, properly constitutes a new branch of spectroscopy. Some of these effects may be observed under

steady-state conditions, requiring only saturation (5); others appear in the transient regime and exhibit interesting coherence properties.

Successive stages of precision in optical spectroscopy for an infrared vibration-rotation spectrum of methane at 3 micrometers are illustrated in Fig. 1. This is the ν_3 vibrational mode, where the four hydrogen atoms move together in opposition to the carbon atom (6). In Fig. 1a (7) the *P*, *Q*, and *R* branch lines can be seen, corresponding to $\Delta J = -1, 0,$ and $+1$, where ΔJ is the change in the rotational angular momentum quantum number *J*. Each line is 24,000 megahertz wide because of instrumental limitations. As the resolution increases, the line labeled *P*(7) breaks up into six lines as indicated in Fig. 1b (8). (Their origin is discussed in the next section.) The line width of each component is 260 Mhz; it results from the molecular gas sample itself through Doppler broadening and is the best resolution that can be achieved by conventional or linear infrared spectroscopy. (We recall that a molecule moving with a velocity component *v* parallel to a light beam of frequency ν produces a frequency shift, the Doppler shift $(\nu/c)v$, where *c* is the speed of light; for a Gaussian distribution in *v*, the line broadens correspondingly.)

Finally, in Fig. 1c (9), a sharp nonlinear spike on a Doppler background is shown for one of these lines, the $F_1^{(2)}$ transition. Here, the width is reduced still another thousandfold because the nonlinearity "selects" molecules in a very narrow velocity band. The Doppler broadening is virtually eliminated, and now only processes that shorten the molecule's interaction time with the optical field—such as molecular collisions or radiative decay—con-

tribute to the remaining width. (Since the transition frequency is uniformly the same for these molecules, the line is said to be "homogeneously" broadened.) The residual width of this spike is 400 kilohertz or approximately 10^{-5} reciprocal centimeters; it is so narrow that the width is determined largely by the molecular transit time through the laser beam. By increasing the diameter of the laser beam or by other means, it may be possible someday to lower this width to the limit set by the spontaneous radiative lifetime, which in the infrared corresponds to about 1000 hertz!

To see such narrow spectral features, the laser light must have a line width even narrower than the profile being examined, and it must be sufficiently intense to induce an appreciable saturation or nonlinearity, requirements that are easily satisfied by many gas lasers. Figure 2 shows a situation where intense monochromatic laser light selects a narrow velocity band by "burning a hole" in the Doppler line shape, thereby depleting the population of the absorbing level (10). Notice that with a single laser this narrow line shape can not be detected as its frequency Ω is tuned, since saturation will occur at every point. The entire line shape including the hole could be monitored, however, with a second laser, a weak monochromatic probe that is tunable. What is needed in Fig. 2 is a mechanism for enhancing the nonlinear response at a particular frequency; that is, a nonlinear resonance condition is required. There now exist several effects of this type which may be utilized for high-resolution spectroscopy, and we consider some of them here.

Lamb Dip

The first example is by Lamb (11), who predicted a power dip in the tuning characteristic of a gas laser—an effect which was quickly verified by experiment (12). The importance of the Lamb dip for high-resolution spectroscopy was not realized until about 1969, however, when successful observations were reported in CH_4 (9),

The author is with the IBM Research Laboratory, San Jose, California 95114. This article is based on lectures that he presented at the "Ettore Majorana" International School of Quantum Electronics, Erice, Sicily, 16 to 29 April 1972.

NH₂D (13), I₂ (14), and SF₆ (15). The effect arises when a molecular sample is excited simultaneously with two oppositely moving laser beams (a standing wave), as shown in Fig. 3. The point is simply that two equally intense laser beams can saturate a sample more readily than one. The only molecules that can interact with both beams are those at the Doppler peak, where the molecular velocity component v is zero and the optical frequency Ω just equals the molecular transition frequency ω . When the laser frequency is detuned from the peak (Ω not equal to ω), one beam saturates the velocity group $+|v|$ and other beam saturates another group $-|v|$; the Doppler shift in each case is the same: $\omega = \Omega (1 - |v|/c)$ for Ω larger than ω . Thus, as the laser frequency is tuned across the Doppler line shape of the absorber, a nonlinear response will not be noticed except at the peak, where it is enhanced because of the interaction of the absorber with the two optical fields. Such dips were first noticed in emission in atomic laser systems, but they can also be monitored in absorption in a sample outside the laser cavity by reflecting the beam back on itself, as noticed in the NH₂D and SF₆ experiments. Still a third variation, due

to Lee and Skolnick (16), is to place the absorbing gas sample inside the laser cavity: Since the sample becomes partially saturated or bleached at its center frequency by the standing wave, the laser output increases correspondingly as in Fig. 1c and shows a spike or inverse dip. We refer to all three effects as Lamb dip resonances since they are so closely related.

A theoretical treatment (11) of the problem shows that the intensity I of the absorbed (or emitted) radiation has a tuning behavior essentially of the form

$$I(\Omega) = g(\Omega) \{1 - 2|\beta|^2 / [(\Omega - \omega)^2 + \gamma^2]\} \quad (1)$$

Here, $g(\Omega)$ is the linear attenuation (or gain) which gives a Doppler-broadened line shape as the laser frequency Ω is tuned about the line center frequency ω . The second term in braces expresses the departure from linearity to the lowest order through the saturation parameter $\beta = (\mu_{10}\epsilon/2\mathcal{K})$, where μ_{10} is the transition dipole matrix element between levels 0 and 1, \mathcal{K} is Planck's constant divided by 2π , and ϵ is the optical field amplitude. This term, on the other hand, has a very narrow tuning range and gives the dip line shape, which has a width γ . The non-

linear signal thus scales as $|\beta/\gamma|^2$ and can be as large as 0.1 even for modest laser power densities of 10 milliwatts per square centimeter, $\mu_{10} = 0.01$ debye, and $\gamma = 1$ Mhz. Because electric dipole matrix elements are rather large in the optical region, the absolute sensitivity of these nonlinear techniques is also high. Signals as small as 1 part in 10⁸ of the laser power can be detected in molecular gases, and this implies millitorr pressures in sample lengths of about 10 cm. It is interesting to note that when molecular collisions determine the line width, a decrease in the molecular density N actually increases the nonlinear signal (which varies as $1/N$) relative to the linear Doppler-broadened background (which is proportional to N). Ultimately, of course, the width becomes independent of N because of the molecular transit time effect or radiative decay.

Equation 1 also predicts that the transition line center can be very accurately located since the dip centers on the transition frequency ω , and the width γ can be very narrow, especially in the infrared.

A Lamb dip resonance obtained by Luntz and Brewer (17) is shown in Fig. 4a for one of the transitions of CH₄ at 3 μ m (18). This is the same line as in Fig. 1b, the rotational E component, but now the line width is about 100 khz full width at half maximum (FWHM) instead of the Doppler width of 260 Mhz. The resolution is thus about 10⁹. The spectrum was obtained by sweeping a stable single frequency continuous-wave (c.w.) 3.39- μ m helium-neon laser, with a CH₄ cell inside the laser cavity, through the CH₄ Doppler line center (see Fig. 5). (The separation between the laser mirrors, which determines the laser frequency, is held fixed by a rigid spacer with a low coefficient of thermal expansion. The entire optical system rests on a massive granite table with an air cushion for acoustic isolation.) With an axial magnetic field, the laser frequency may be tuned about 3 gigahertz into near coincidence with the CH₄ transition frequency, within the Doppler width, while a fine frequency sweep for seeing the dip is provided by a piezoelectric scan of the laser cavity length. Derivative line shape resonances are observed as a change in laser output by using weak audio modulation of the cavity length and phase sensitive detection. In principle, the Ne atoms will also yield a Lamb dip, but it is so broad and weak because of the

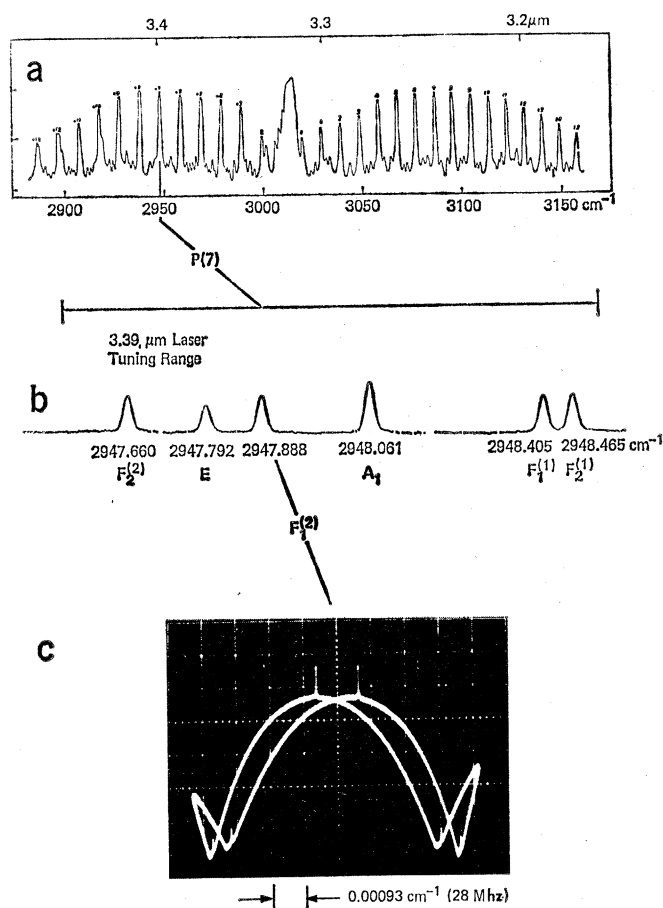


Fig. 1. The ν_3 vibration-rotation band of CH₄ at 3.3 μ m. (a) Low-resolution absorption spectrum. Each line is 24,000 Mhz wide (7). (b) A higher-resolution absorption spectrum showing the $P(7)$ rotational fine structure. Each line is 260 Mhz wide because of Doppler broadening (8). (c) A nonlinear spectrum of the $F_1^{(2)}$ line. It is obtained by monitoring the output of a 3.39- μ m He-Ne laser, which contains a CH₄ sample inside its optical cavity, as the laser frequency is tuned. The nonlinear spike 400 khz wide (homogeneous broadening) occurs on the Doppler background at its peak (9).

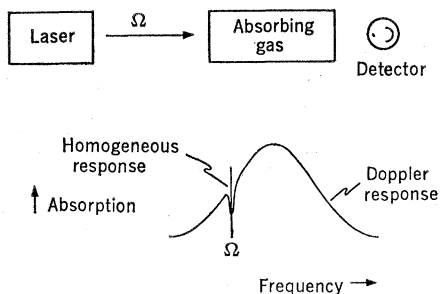


Fig. 2. "Hole burning" of a Doppler-broadened transition as indicated by an absorption dip centered on the laser frequency Ω .

high-pressure (10 torr) discharge that it is not evident. The CH_4 sample, which is at a low pressure of about 1 mtorr, thus acts as an exceedingly narrow band-pass filter which increases the output within its Lamb dip but reduces the output at neighboring frequencies.

At this degree of resolution, one can now attempt to do experiments that were impossible heretofore. As an example, Fig. 4b shows how the Lamb dip spectrum is modified when an electric field of only 1660 volts per centimeter is applied to the CH_4 sample. The line splits into 13 equally spaced and completely resolved components, all falling within 20 Mhz or one-tenth of the Doppler width. The number of lines confirms unambiguously that the upper rotational state of this transition has angular momentum quantum number J equal to 6, in agreement with its $P(7)$ transition assignment. Moreover, the result verifies for the first time an old theory of Mizushima and Venkateswarlu (19), that spherical top molecules like CH_4 can exhibit a small dipole moment in the excited ν_3 vibrational state and thus a first-order Stark effect. This is due to a vibrational anharmonicity which removes the three-fold vibrational degeneracy of the ν_3 mode; it also produces the rotational splittings of Fig. 1b.

Note that the magnitude of this induced dipole moment cannot be ascertained from the Lamb dip results as there is no frequency scale. However, the optical double-resonance technique (described below) gives a dipole moment of 0.0200 ± 0.0001 debye (17), which, although quite small, can be determined with considerable precision. Thus, the observation of even a single molecular transition under high resolution can yield a variety of significant results. In addition, many other organic molecules have been studied by Luntz and Brewer (17) with the magnetically

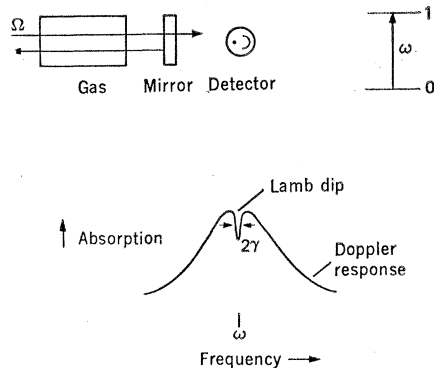


Fig. 3. Experimental arrangement for observing standing wave or Lamb dip resonances in an absorbing gas sample excited by laser radiation of frequency Ω . The frequency of molecular transitions between energy levels 0 and 1 is ω ; the width of the Lamb dip line shape is 2γ .

tuned 3.39- μm He-Ne laser, since they all have C-H vibrational modes in this region and the density of lines is high, even in a tuning range of 6 Ghz.

Narrow hyperfine splittings, which result from nuclear interactions, also have been observed for the first time in molecular spectra in the visible region. Using the standing wave saturation technique, Hanes *et al.* (14) were able to observe hyperfine structure for a transition of I_2 with a frequency overlapping the optical frequency of the 0.633- μm He-Ne laser. An I_2 spectrum of this type obtained by Hänsch, Levenson, and Schawlow (20) is shown in Fig. 6 (21). This spectrum reveals all 21 hyperfine components predicted for a model that includes nuclear electric quadrupole and magnetic hyperfine interactions. From the experimental fit, the strength of these interactions can now be determined quantitatively.

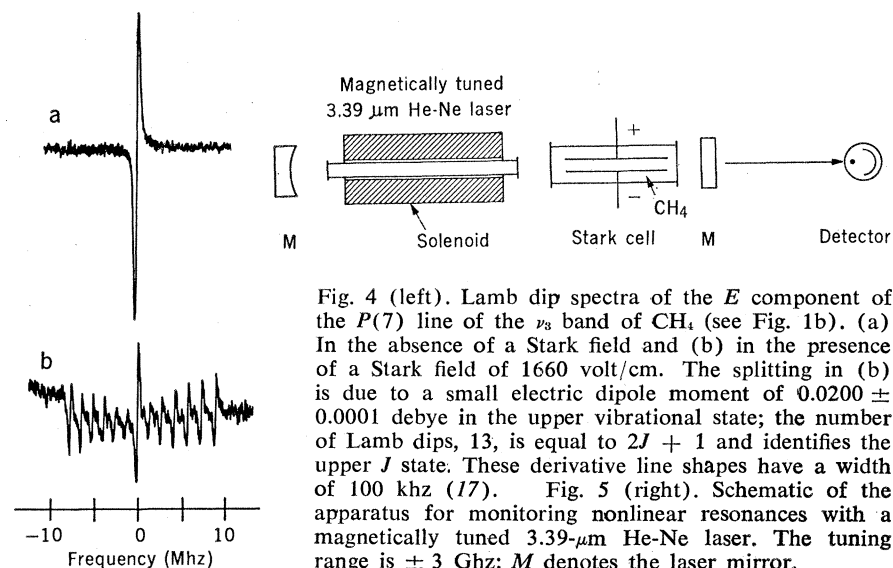


Fig. 4 (left). Lamb dip spectra of the E component of the $P(7)$ line of the ν_3 band of CH_4 (see Fig. 1b). (a) In the absence of a Stark field and (b) in the presence of a Stark field of 1660 volt/cm. The splitting in (b) is due to a small electric dipole moment of 0.0200 ± 0.0001 debye in the upper vibrational state; the number of Lamb dips, 13, is equal to $2J + 1$ and identifies the upper J state. These derivative line shapes have a width of 100 khz (17). Fig. 5 (right). Schematic of the apparatus for monitoring nonlinear resonances with a magnetically tuned 3.39- μm He-Ne laser. The tuning range is ± 3 Ghz; M denotes the laser mirror.

Fundamental Constants

Another spectacular application of the Lamb dip is in precision measurements of length (wavelength) and time (frequency), that is, in the area of metrology. Using a CH_4 cell inside the cavity of a 3.39- μm He-Ne laser, Barger and Hall (9) stabilized the frequency of this laser with a servo loop locked to the CH_4 Lamb dip. The experimental arrangement resembles Fig. 5, but in addition the detector output drives the laser frequency to the center of the Lamb dip by piezoelectric cavity tuning. Since the dip appears as a derivative line shape, as above, a stable point is reached at its peak, where the derivative is zero. In this case, the CH_4 transition $F_1^{(2)}$, shown in Fig. 1c, is monitored. A laser frequency stability of 1 part in 10^{13} has been achieved, and the CH_4 line center can be reproduced in independent lasers to 1 part in 10^{11} . Sources of this stability are quite attractive as optical wavelength or frequency standards, especially since the primary length standard, the krypton-86 line at 6057 angstroms, is accurate to 1 part in 10^8 .

Evenson *et al.* (22) have measured the absolute frequency of the 3.39- μm He-Ne laser stabilized with CH_4 , the highest frequency ever measured, by using a chain of lasers and klystrons with frequencies extending down to the cesium beam frequency standard (23). The detection method of laser harmonic frequency mixing, which is due to Javan *et al.* (24, 25) involves a point contact junction (a cat's whisker device) in which laser and microwave radiation mix to produce harmonics and a zero or low-frequency beat signal.

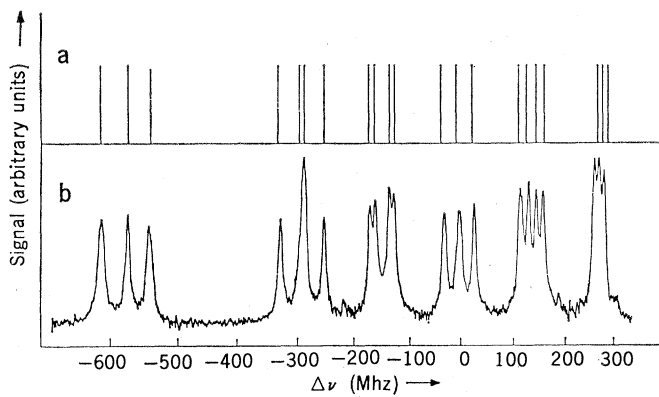


Fig. 6. Hyperfine structure of an electronic transition of $^{127}\text{I}_2$ in the visible, obtained by the Lamb dip resonance technique. (a) Theoretical spectrum and (b) observed spectrum. The transition, a $P(117)$ line of the 21-1 band of $X \rightarrow B$, is excited by a krypton-ion laser at $0.5682 \mu\text{m}$. The line positions are given by $\Delta\nu$ (20).

For example, in the first step in the chain a far-infrared hydrogen cyanide laser beam at $337 \mu\text{m}$ mixes with the twelfth harmonic of a klystron (24). Frequency measurements at $3.39 \mu\text{m}$ in combination with an interferometric wavelength measurement now provide a value for the speed of light, $2.99792460(6) \times 10^{10}$ centimeters per second, which increases the present accuracy by about one order of magnitude (23). Since frequency can be determined more accurately than wavelength, the speed of light may ultimately be a defined quantity that links wavelength to a frequency measurement.

An interesting variation of these laser stabilization techniques has been developed by Freed and Javan (26). They locked the frequency of a $10.6\text{-}\mu\text{m}$ carbon dioxide laser, which is part of the optical chain mentioned above,

to the standing wave saturation resonance of a CO_2 sample at low pressure and room temperature, inside the laser cavity. Since the lower level of these transitions is not the ground vibrational state, the dip is observed by spontaneous emission at $4.3 \mu\text{m}$ ($001 \rightarrow 000$) rather than by weak absorption at $10.6 \mu\text{m}$ ($100 \rightarrow 001$). This procedure eliminates the laser background and thus increases the detection sensitivity; moreover, it allows one to preselect any of the laser transitions in the P and R branches as an optical frequency standard.

Frequency-stabilized lasers also can be used to investigate the mode spectrum of the earth at frequencies as low as a few cycles per hour, as well as other geophysical problems. A $3.39\text{-}\mu\text{m}$ He-Ne laser stabilized with CH_4 has been used to produce a beat signal with a

second He-Ne laser, locked to a 30-meter Fabry-Perot interferometer (27). Length variations in the large interferometer resulting from strains in the earth translate as variations in the beat frequency. Because of the high stability, slowly varying changes in length can be readily monitored, and the mechanical calibration problem associated with older methods is avoided.

Optical Double Resonance and Level Crossing

A second type of nonlinear resonance can occur when a molecule is irradiated by two optical fields of different frequencies. This is also a powerful spectroscopic technique, capable of resolving small splittings that fall within the Doppler width. Double-resonance spectroscopy is, of course, a familiar technique in the microwave and radio-frequency regions as well as in optical pumping, but it is only recently that the analog has been carried out with two optical frequencies. Here, two optical transitions sharing a common level interact simultaneously with two optical fields. Figure 7 shows the level structure and the experimental arrangement. Molecules that are driven by both optical fields can pass, for example, from level 2 to level 1 by absorption of a photon of frequency Ω_2 and by emission of a photon of frequency Ω_1 —a process that exhibits a nonlinear

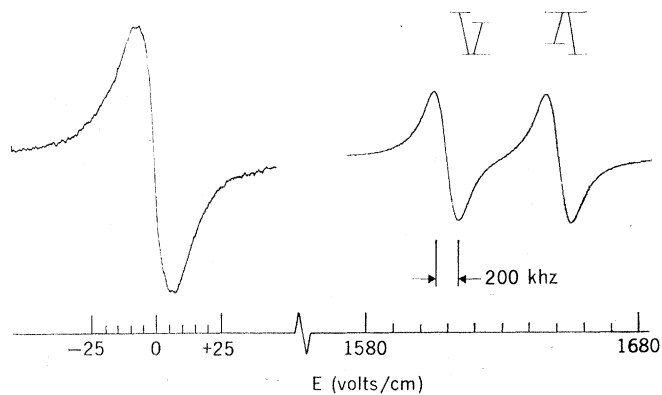
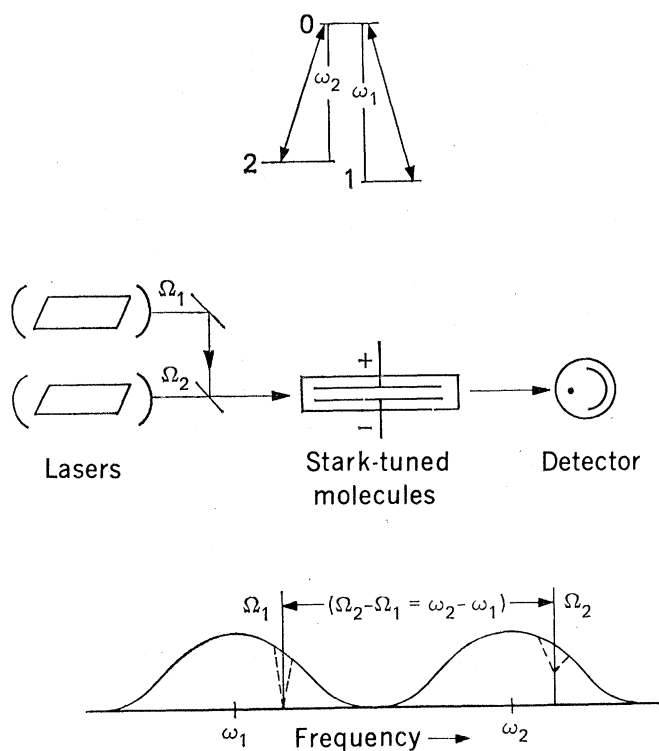


Fig. 7 (left). Schematic of the optical double-resonance technique, showing the level structure, experimental arrangement, and tuning behavior. The two transitions are in close proximity, and their Doppler line shapes may even overlap (30). The transition frequencies are ω_1 and ω_2 , and the optical frequencies are Ω_1 and Ω_2 . Fig. 8 (right). Stark-tuned optical double-resonance spectrum of $^{12}\text{CH}_3\text{F}$. The infrared ν_3 band line is due to the transition $(\nu_3, J, K) = (0, 12, 2) \rightarrow (1, 12, 2)$. The excitation was by two CO_2 lasers at $9.6 \mu\text{m}$ and with a frequency difference $\Omega_1 - \Omega_2$ equal to 39.629 Mhz . Nonlinear resonances appear as the Stark field E is swept (30).

intensity dependence similar to that in Eq. 1 (28). For two overlapping Doppler-broadened transitions, a molecule will interact in this way only if the Doppler shift is the same for each field, or $\Omega_1 - \omega_1 = \Omega_2 - \omega_2$.

Thus, if one of the laser frequencies is varied or if the molecular-level splitting $\omega_1 - \omega_2$ is tuned by the Zeeman or Stark effect, a nonlinear response will appear for the resonance condition $\Omega_2 - \Omega_1 = \omega_2 - \omega_1$. Note that this is similar to the Lamb dip since one velocity group must interact simultaneously with two radiation fields at resonance, but, off resonance, the nonlinear interaction is with only one field and is therefore reduced. Since only a single narrow velocity group is monitored, its resonance line shape will be homogeneously broadened and, again, it may be orders of magnitude narrower than the Doppler width.

An experiment of this type was first demonstrated by Schlossberg and Javan (29) for xenon, by using a multimode Zeeman-tuned Xe laser. The technique has been extended to molecules (30–32), especially to the 10- and 3- μm bands of CH_3F . This symmetric top molecule has a permanent electric dipole moment μ and exhibits a first-order Stark effect in an external field E , so that the nonlinear resonance condition becomes

$$\Omega_1 - \Omega_2 = 2\mu EK/[J(J+1)h] \quad (2)$$

Once the rotational assignment (J, K) is known, this relation permits an optical determination of the dipole moment.

Figure 8 shows a double-resonance spectrum for CH_3F , obtained by Brewer (30) by using two 10- μm c.w. CO_2 lasers and sweeping the Stark field. The beat frequency ($\Omega_1 - \Omega_2$) is held fixed to a stability of 3 parts in 10^6 by locking one laser to the other in a servo loop that compares this frequency to a reference. The beat, which is easily measured with a photodetector and a counter, provides an accurate frequency scale for the spectrum. Since the dipole moments of ground and excited vibrational states are slightly different, there are two such resonance signals. These appear near 1600 volt/cm in Fig. 8, and, although they are separated by only about 1 Mhz, they are clearly resolved since the line width is only 100 khz half width at half maximum. Here, the magnitude of the Stark tuning rate itself is a critical test of the transition assignment and it yields $(v_3, J, K) = (0, 12, 2) \rightarrow (1, 12, 2)$ for this v_3 vibrational line. With this

Table 1. Electric dipole moment of CH_3F for ground and excited vibrational states; v, J , and K are quantum numbers of the vibration-rotation states. The numbers in parentheses after the dipole moment values are the uncertainties in the last digits.

v	J	K	Dipole moment (debye)	Spectroscopic technique	Reference
0	0,1,2	0,1	1.8576 (10)	Microwave	(58)
0	1	1	1.8580 (4)	Molecular beam	(59)
0	5	4	1.85852 (11)	Molecular beam	(59)
0	4	3	1.8578 (6)*	Nonlinear	(31)
0	12	2	1.8596 (4)	Nonlinear	(31)
0	10	6	1.854 (4)†	Nonlinear	(32)
$v_3 = 1$	5	3	1.9038 (6)*	Nonlinear	(31)
$v_3 = 1$	12	2	1.9067 (4)	Nonlinear	(31)
$v_1 = 1$	9	6	1.834 (4)†	Nonlinear	(32)

* Data for $^{13}\text{CH}_3\text{F}$; the other entries are for $^{12}\text{CH}_3\text{F}$. † The source was a 3.39- μm He-Ne laser; for the other entries CO_2 lasers at 9 to 10 μm were used.

information, it is possible to obtain highly precise values of the dipole moment for both ground and excited vibrational states with equal ease. In Table 1 the results at 10 μm are summarized and similar measurements of the v_1 vibration at 3.39 μm are compared. At this resolution, even the small change of 0.001 debye due to rotational distortion is observable, and, because of the high sensitivity, isotopic species such as $^{13}\text{CH}_3\text{F}$ (1 percent abun-

dant) can be observed in natural abundance. It should be noted from Table 1 that the older spectroscopic techniques of microwave and molecular beam resonance cannot probe these excited vibrational and rotational states, either because the Boltzmann population is too small or because the rotational transitions fall in the far infrared.

Returning to the first spectral feature of Fig. 8, which is centered on zero Stark field, we see that this is simply a degenerate case of optical double resonance. The resonance condition now becomes $\omega_1 - \omega_2 = 0$ and the resonance signal can be observed with a single-frequency source. This zero-field level crossing (33) superficially resembles the well-known Hanle effect, in which crossings are monitored linearly through spontaneous emission. However, the signal in Fig. 8 involves a nonlinear absorption and is not limited to crossings between excited states characterized by a fast radiative decay rate.

Still another molecular level-crossing effect, developed by Luntz (34), may be observed with Stark tuning when a nonresonant radio-frequency field is applied simultaneously across the Stark plates. The radio-frequency field modulates the molecule, producing sidebands in its level structure which are displaced from the parent levels by the radio frequency (see Fig. 9). With Stark tuning, the sideband and parent levels cross; the resonance condition is the same as in the double-resonance case. The signal is nonlinear because it depends on both the radio-frequency and optical intensities. These level crossings have been observed in CH_4 ; they yield the same dipole moment as does the double-resonance technique, and their intensity is predicted by the

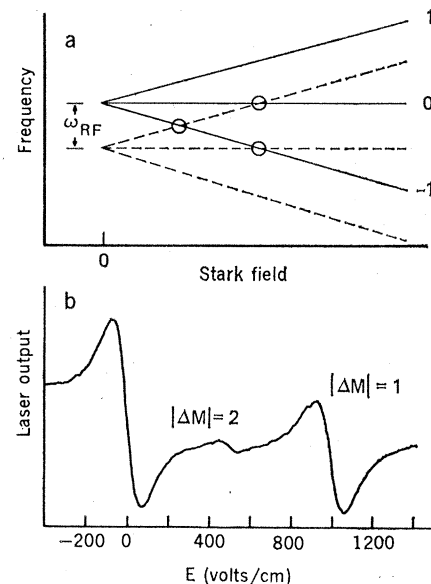


Fig. 9. Radio-frequency induced level crossing in CH_4 (the E line of Fig. 1b). (a) The level crossings for $\Delta M = 1$ and $\Delta M = 2$ are indicated by circles. For simplicity, only one radio-frequency sideband (dashed lines) and only the lowest M levels are shown. The radio frequency is ω_{RF} . (b) Spectrum obtained by monitoring the output of a 3.39- μm He-Ne laser when the CH_4 sample is swept by the Stark field (E) and the radio-frequency Stark field is 0.8447 Mhz. The arrangement is similar to that in Fig. 5 (34).

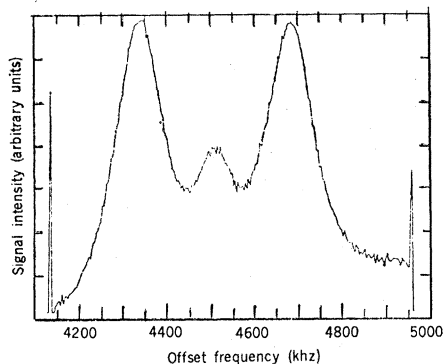


Fig. 10. Standing wave resonances in Zeeman sublevels of the $F_1^{(2)}$ line of CH_4 (Fig. 1b); the magnetic field is 670 gauss. The output of a $3.39\text{-}\mu\text{m}$ He-Ne laser with an internal CH_4 cell is monitored as the laser frequency is swept. One side peak is due to a transition with $\Delta M = +1$, the other to a transition with $\Delta M = -1$; the central peak corresponds to the crossover resonance resulting from the simultaneously coupled transitions $\Delta M = +1$ and $\Delta M = -1$ (38).

Autler-Townes theory (35). The effect is quite similar to that observed in optical pumping studies of atoms "dressed" by radio-frequency magnetic fields (36), and is a useful alternate method for obtaining narrow resonances.

Zeeman Studies

The magnetic properties or Zeeman effect in ordinary molecules (in ground or $^1\Sigma$ states) can also be examined with these techniques, even though the magnetic moments are extremely small,

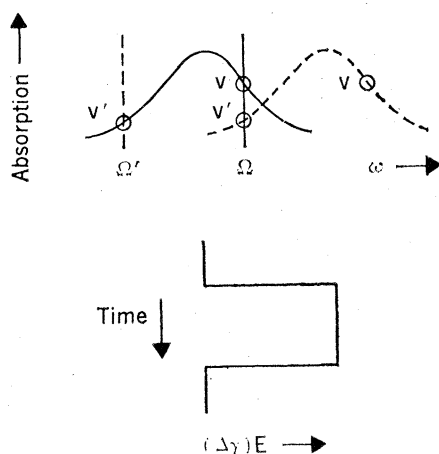


Fig. 12. Optical switching behavior of a Doppler-broadened transition when a Stark pulse of amplitude E is applied. The Stark shift is $(\Delta\gamma)E$, the laser frequency is Ω , and coherent emission can occur at Ω' , for example. The molecular transition frequency is ω ; the molecular velocities are v and v' .

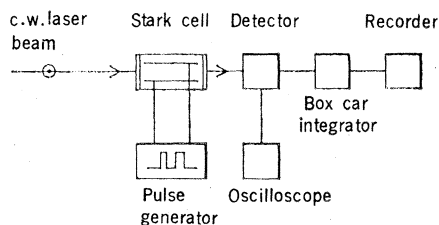


Fig. 11. Schematic of a simple technique for observing coherent optical transient signals with a c.w. laser beam and one or more Stark pulses (44).

typically a fraction of a nuclear magneton. In the past, only microwave and molecular beam resonance spectroscopy have been capable of this resolution. Using the zero-field level crossing effect, Luntz and Brewer (37) observed a resonance by magnetically tuning the $F_1^{(2)}$ line of CH_4 at $3.39\ \mu\text{m}$ and obtained 0.36 ± 0.07 nuclear magnetons for the rotational magnetic moment in its ground and excited vibrational states. This value has been improved in Lamp dip studies by Uzgiris, Hall, and Barger (38) who found $+0.311 \pm 0.006$ for $v_3 = 0$ and 1, the sign being positive. By comparison the molecular beam result (39), which applies only to $v_3 = 0$, is 0.3133 ± 0.0002 , with undetermined sign. These laser experiments are the first examples of optical measurements with sufficient resolution to detect the magnetic tuning behavior of $^1\Sigma$ molecules.

Uzgiris *et al.* (38) also observed another interesting nonlinear resonance

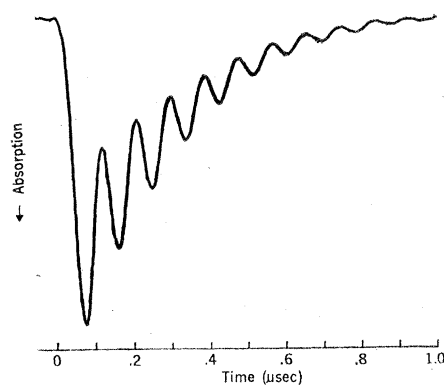


Fig. 13. Optical free induction decay in NH_2D . The molecular sample has been prepared in steady state by a c.w. beam of $10.6\text{-}\mu\text{m}$ radiation from a CO_2 laser and freely radiates an intense, coherent, directional beam when it is suddenly switched out of resonance by a Stark field. The beat frequency is the Stark shift, and it arises because the emission heterodynes with the collinear laser beam. The slowly varying background is a nutation signal, which is more clearly shown in Fig. 14. The transition is $(v_3, J, M) = (1, 5, 4) \rightarrow (0, 4, 3)$ (46).

effect, a crossover resonance, which had been predicted by Schlossberg and Javan (40). It arises when two closely spaced levels, in this case Zeeman M sublevels, are simultaneously coupled to a third common level by a standing wave optical field. As the laser frequency is tuned, each transition will produce a Lamb dip and, in addition, a third weaker dip midway between the other two, as shown in Fig. 10. This extra resonance is due to a particular axial velocity group (55 cm/sec) that can simultaneously shift into resonance one traveling wave with one transition and the oppositely moving wave with the second transition.

Atoms

A versatile technique for observing nonlinear resonances in the visible has been developed by Hänsch, Shahin, and Schawlow (41) and applied to atoms. The source is a repetitively pulsed dye laser which is continuously tunable, greatly extending the number of transitions which can be examined in this spectral region. Pulse expansion in a Fabry-Perot interferometer outside the laser cavity reduces the line width from 300 to 7 Mhz. A saturating beam and a probe beam derived from the laser traverse the same sample volume, but from opposite directions, as in the Lamp dip studies described above. With this technique, the hyperfine structure of the sodium D lines was resolved with line widths of 40 Mhz FWHM. In contrast, the limiting width due to radiative decay is 20 Mhz and the Doppler width is about 1300 Mhz. In addition, the crossover resonances mentioned above appeared, and by delaying the probe pulse after saturation, the restoration of equilibrium was followed for 100 nanoseconds in the presence of argon buffer gas.

Using the same method, these authors also resolved for the first time single fine-structure components of the hydrogen atom H_α Balmer line at $6563\ \text{\AA}$, bypassing the Doppler width of about 6000 Mhz (42). They obtained line widths of 250 to 300 Mhz FWHM, about one order of magnitude narrower than the best previous value. This makes possible direct observation of the Lamb shift in the $n = 2$ state. In addition, following a suggestion of Series (43), they proposed that the Rydberg constant might be determined to high precision, one part in 2×10^8 , by using these nonlinear resonances.

Coherent Transients

Thus far, our discussion has centered on measurements under steady-state conditions, and the dynamic as well as the coherent aspects of these nonlinear optical interactions have been neglected. Numerous examples of coherent transient effects can be found at radio frequencies in nuclear magnetic resonance (NMR), where such methods have provided an abundance of information on relaxation phenomena and high-resolution spectra (3). Until now these effects have not been particularly useful for optical spectroscopy because of the difficulties associated with pulsed laser sources. Using a new approach to the subject, Brewer and Shoemaker (44) recently developed a simple method for examining such transient behavior in the optical region and even for examining new phenomena that have no analog in NMR. Whereas previous laser studies required the use of a pulsed source, they utilized a c.w. laser and pulsed the level splitting of the absorbing molecule by the Stark effect. Transient optical signals are readily seen in transmission by electronically gating the optical absorption with a pulsed electric field. The experimental arrangement is shown in Fig. 11 and the switching principle in Fig. 12. Interestingly enough, the same principle could have been applied to microwave spectroscopy, prior to lasers, many years ago. In fact, these coherent transient effects do occur in all microwave spectrometers that utilize square-wave Stark fields, and they have gone unnoticed for over 20 years!

In Fig. 12, we consider a simple two-level system which exhibits a change in transition frequency when a Stark pulse of amplitude E is applied. Initially, molecules of velocity v are excited in steady state by laser light of frequency Ω , but when the pulse appears this group is no longer in resonance and will begin to radiate, by analogy with NMR (45), a free induction decay signal (Fig. 13) (46). This emission appears as a heterodyne beat signal, as described below. At the same time, a second velocity group v' will be switched into resonance and will alternately absorb and emit radiation. This optical ringing or nutation effect shows up as a damped oscillation (Fig. 14) (44). Finally, when the pulse terminates, the group v is suddenly excited and it too begins to nutate, while the group v' now emits a free induction signal.

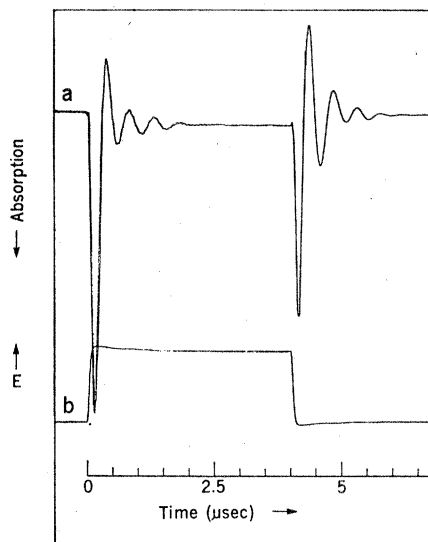


Fig. 14. (a) Optical nutation in $^{13}\text{CH}_3\text{F}$ following (b) a Stark pulse of amplitude E . The nutation period gives the effective saturation parameter ($\mu\epsilon/\hbar$) directly. The excitation was by a c.w. $9.6\text{-}\mu\text{m}$ CO_2 laser, and the transition is $(v_3, J, K) = (0, 4, 3) \rightarrow (1, 5, 3)$. The various free induction decay beats that are possible here do not appear because of their mutual interference and rapid decay (44).

If two Stark pulses are applied, as illustrated in Fig. 15, it is possible to observe a photon echo (44), the optical analog of a spin echo (47). [Photon echoes were first demonstrated by Kurnit, Abella, and Hartmann (48), who used a pulsed ruby laser source and a ruby sample.] The first Stark pulse switches the velocity group v' into resonance with the optical field; this induces a macroscopic electric dipole moment. The transition levels are thus in a superposition state. When the pulse ends, the induced dipoles begin to get out of phase because of a spread in the transition frequencies. This is due to the finite pulse width τ , which picks out Fourier components given roughly by $(\Omega \pm 1/\tau)$ within the Doppler line shape. The interference is destructive and causes the free induction decay signal to be short-lived. However, a second pulse lasting twice as long as the first now reverses the direction of the dipoles and brings them into phase again in just the amount of time that elapsed between the first two pulses. At this point the dipoles interfere constructively, and the sample spontaneously emits a pulse of light—the photon echo.

The laser beam prepares a sample with a macroscopic moment, a phased array of dipoles, which can radiate in unison only in the forward direction.

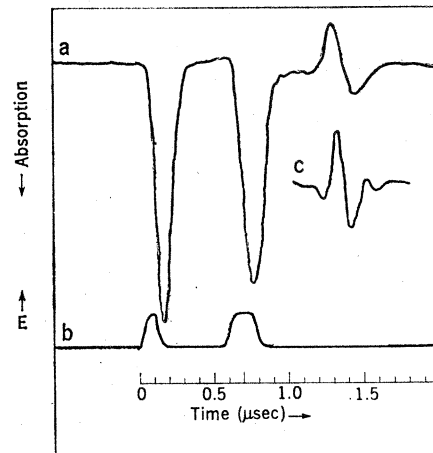


Fig. 15. (a) Photon echoes in $^{13}\text{CH}_3\text{F}$ at $9.6\text{-}\mu\text{m}$ following (b) two Stark pulses of amplitude E . In (c) the beat frequency of the echo signal has increased over its value in (a) because the amplitude of the Stark pulse has almost doubled (to 60 volt/cm) (44).

The emission due to the echo or free induction decay, therefore, propagates together with the laser beam and produces at the detector a heterodyne beat $(\Omega' - \Omega)$ whose frequency is the Stark shift. Heterodyne detection enhances the sensitivity 1000-fold; it occurs because the sample is prepared when the pulse is on (off) and emits with a shifted frequency when the pulse is off (on).

The echo amplitude ϵ will, of course, decay with an increasing pulse interval τ_s because of molecular collisions or other effects which disrupt their coherence. From the decay envelope $\epsilon/\epsilon_0 = \exp(-2\tau_s/T_2)$, where ϵ_0 is the amplitude for a zero time delay, one can obtain the homogeneous relaxation time T_2 and begin to investigate the relaxation properties of molecular systems in specific quantum states, without the power broadening present in steady-state measurements.

Still another effect, which Shoemaker and Brewer (49) call "two-photon superradiance," is seen when a c.w. laser beam excites a molecular sample whose level degeneracy is suddenly removed by a Stark field. In this case, the corresponding analog in NMR is unknown. Coherent excitation places the initially degenerate levels in a correlated or superposition state which remembers its preparation after the Stark field is applied. With the degeneracy removed, the various transitions will then be out of resonance with the laser frequency, and several free induction decay signals will follow. In addition, a two-photon or Raman-like process can take place where laser light scat-

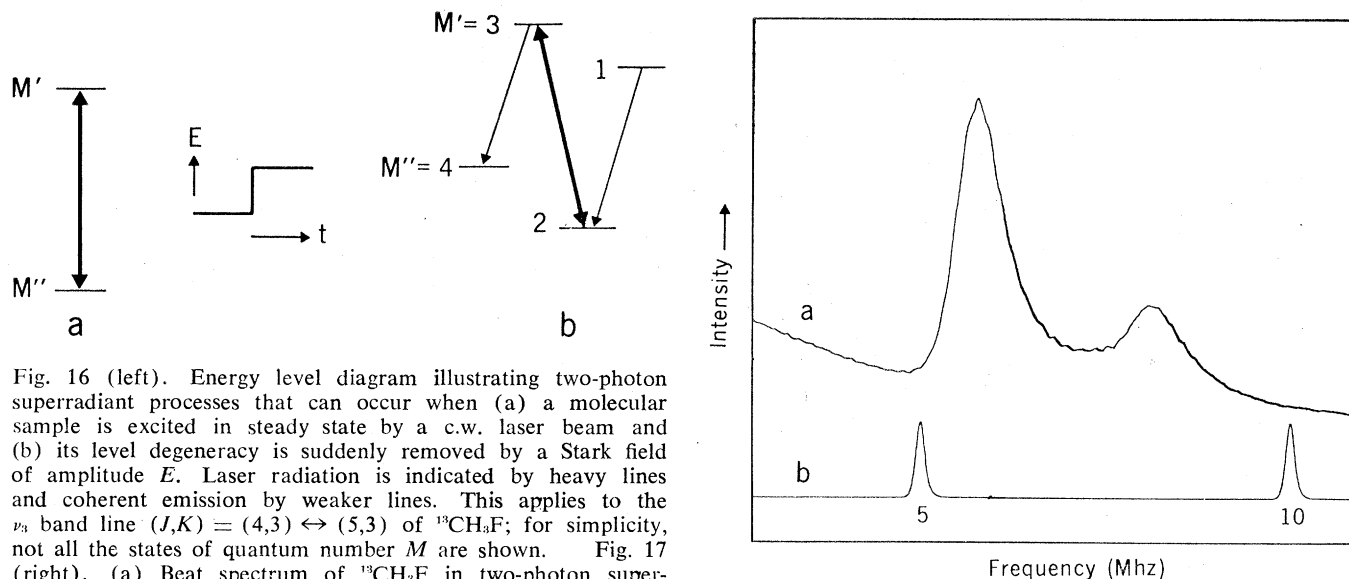


Fig. 16 (left). Energy level diagram illustrating two-photon superradiant processes that can occur when (a) a molecular sample is excited in steady state by a c.w. laser beam and (b) its level degeneracy is suddenly removed by a Stark field of amplitude E . Laser radiation is indicated by heavy lines and coherent emission by weaker lines. This applies to the ν_3 band line $(J,K) = (4,3) \leftrightarrow (5,3)$ of $^{13}\text{CH}_3\text{F}$; for simplicity, not all the states of quantum number M are shown. Fig. 17 (right). (a) Beat spectrum of $^{13}\text{CH}_3\text{F}$ in two-photon superradiance. The low-frequency component is ω_{m_1} , and the other component is ω_{m_2} (see Fig. 16). (b) Frequency calibration. The transitions were excited with a c.w. 9.6- μm CO_2 laser, and the transient beat signals were detected with a spectrum analyzer and displayed on an X-Y recorder (49).

ters, in the forward direction, off the coherently prepared sample. This is indicated in Fig. 16, where a laser photon of frequency ν_1 is absorbed and another of a different frequency ν_2 is emitted, all the molecules doing this together in phase. The emission again heterodynes with the laser beam and, when detected by a spectrum analyzer, shows two beats (Fig. 17) corresponding to the splittings between levels 2 and 4 and levels 1 and 3 in Fig. 16. Note that the effect disappears if the preparation is destroyed, for example, by an initial Stark bias field. Thus, the process resembles Dicke's superradiance (50).

Another interesting property is that the two-photon process outlives the free induction decay signals and decays with a relaxation time T_2 , as in the photon echo. This is because Doppler dephasing effects are absent in two-photon forward scattering, since the Doppler shift, given by $(v/c)(\nu_1 - \nu_2)$, is only about 10 hertz. For free induction decay, a one-photon process, $(v/c)v$ is approximately 60 Mhz in the infrared, and the decay is short-lived.

The two-photon effect provides spectral information similar to that obtained in the optical double-resonance experiments and has the advantage of requiring only one laser. Hence, this transient technique provides a new kind of Fourier transform spectroscopy.

Tunable Lasers

Nonlinear spectroscopy will, of course, develop more rapidly as stable tunable lasers become more available.

A desirable source might have a spectral width of approximately 10 khz, an output power density in the range 10 to 1000 mwatt/cm², and a broad range of tunability, perhaps 10 percent of the center frequency. Many gas lasers satisfy the first two requirements, but not the third. The 10- μm CO_2 laser, for example, has about 70 lines covering 100 cm^{-1} , an intrinsic line width of less than 1 hertz, and an absolute stability of about 100 hertz, but each line can be tuned only over the Doppler width of 50 Mhz.

Semiconductor diode lasers (51), such as $\text{Pb}_{1-x}\text{Sn}_x\text{Te}$, possess a band width of 50 khz; by varying x they can be made to emit anywhere in the range 6.5 to 32 μm , and they can be fine-tuned by a small change in diode current, in some cases over 40 cm^{-1} . They suffer, however, from having an output of less than a milliwatt, a 50 percent loss in the tuning range due to mode hopping, and a wide divergence angle because of their small dimensions (about 1 cubic millimeter).

In the visible, the pulsed dye laser has already been used successfully in nonlinear spectroscopy (41, 42). Because the radiative lifetimes in this region and in the near ultraviolet imply widths of approximately 100 Mhz, the line width and frequently stability of the laser are not as critical as in the infrared. The c.w. dye laser (52) may also be useful in these studies if the problems of amplitude and frequency stability are solved. Similarly, the parametric oscillator (53) lacks adequate frequency stability at present, although it can be tuned from the near infrared to the near ultraviolet.

The spin-flip Raman laser (54-56), first developed by Patel and Shaw (54), apparently possesses all three requirements: a line width of less than 1 khz, an output power of approximately 1 watt, and a tuning range of 5.7 to 6.2 μm . However, for Lamb dip studies absolute frequency stability may limit the line width to about 1 Mhz because of thermal drift in the InSb Raman sample.

Oka and Shimizu (57) have developed still another technique which shows promise as a tunable source, even though it is not a laser. They combine microwave and infrared laser radiation in a two-photon molecular transition. For each laser frequency ν_1 , which is fixed, the klystron frequency ν_2 may be tuned throughout the microwave band so that accessible transitions appear at $\nu_1 \pm \nu_2$. However, this process is not velocity selective, and to obtain lines narrower than the Doppler width an additional nonlinear effect, such as the Lamb dip effect, must be applied.

Conclusion

Although nonlinear spectroscopy evolved slowly in its initial stages, it is now becoming an important new branch of atomic and molecular spectroscopy. A variety of phenomena are being observed for the first time, either in steady state or in transient behavior. In a sense, the methods of microwave and nuclear magnetic resonance spectroscopy are now being reproduced in the optical region, and with the same precision and detail.

References and Notes

- C. H. Townes and A. L. Schawlow, *Micro-wave Spectroscopy* (McGraw-Hill, New York, 1955).
- N. F. Ramsey, *Molecular Beams* (Oxford Univ. Press, London, 1956).
- A. Abragam, *The Principles of Nuclear Magnetism* (Oxford Univ. Press, London, 1961).
- A. Kastler, *Science* **158**, 214 (1967).
- K. Shimoda and T. Shimizu, *Progress in Quantum Electronics* (Pergamon, New York, in press). This is a review article on non-linear spectroscopy which covers certain aspects of saturation phenomena.
- G. Herzberg, *Molecular Spectra and Molecular Structure* (Van Nostrand, New York, 1966), p. 100.
- A. H. Nielsen and H. H. Nielsen, *Phys. Rev.* **48**, 864 (1935).
- E. K. Plyler, private communication.
- R. L. Barger and J. L. Hall, *Phys. Rev. Lett.* **22**, 4 (1969).
- W. R. Bennett, Jr., *Phys. Rev.* **126**, 580 (1962).
- W. E. Lamb, Jr., *ibid.* **134**, A1429 (1964). The main results of the paper were reported at the Third International Conference on Quantum Electronics, Paris, February 1963. Lectures on some of the material were given at the 1963 Varenna summer school.
- A. Szoke and A. Javan, *Phys. Rev. Lett.* **10**, 521 (1963); R. A. McFarlane, W. R. Bennett, W. E. Lamb, Jr., *Appl. Phys. Lett.* **2**, 189 (1963).
- R. G. Brewer, M. J. Kelly, A. Javan, *Phys. Rev. Lett.* **23**, 559 (1969).
- G. R. Hanes and C. E. Dahlstrom, *Appl. Phys. Lett.* **14**, 362 (1969); G. R. Hanes and K. M. Baird, *Metrologia* **5**, 32 (1969).
- P. Rabinowitz, R. Keller, J. T. LaTourrette, *Appl. Phys. Lett.* **14**, 376 (1969); F. Shimizu, *ibid.*, p. 378; N. G. Basov, I. N. Kompanets, O. N. Kompanets, V. S. Letokhov, V. V. Nikitin, *Sov. Phys. JETP Lett.* **9**, 345 (1969).
- P. H. Lee and M. L. Skolnick, *Appl. Phys. Lett.* **10**, 303 (1967).
- A. C. Luntz and R. G. Brewer, *J. Chem. Phys.* **54**, 3641 (1971).
- For linear absorption see K. Uehara, K. Sakurai, K. Shimoda, *J. Phys. Soc. Japan* **26**, 1018 (1969).
- M. Mizushima and P. Venkateswarlu, *J. Chem. Phys.* **21**, 705 (1953).
- T. W. Hänsch, M. D. Levenson, A. L. Schawlow, *Phys. Rev. Lett.* **26**, 946 (1971).
- See also M. D. Levenson and A. L. Schawlow, *Phys. Rev.*, in press.
- K. M. Evenson, G. W. Day, J. S. Wells, L. O. Mullen, *Appl. Phys. Lett.* **20**, 133 (1972).
- R. L. Barger, J. D. Cupp, B. L. Danielson, G. W. Day, K. M. Evenson, J. L. Hall, D. G. McDonald, L. O. Mullen, F. R. Petersen, A. S. Risley, J. S. Wells, paper presented at the 7th International Quantum Electronics Conference, Montreal, 1972.
- L. O. Hocker, A. Javan, D. Rao, L. Frenkel, T. Sullivan, *Appl. Phys. Lett.* **20**, 147 (1972).
- A. Javan, *Ann. N.Y. Acad. Sci.* **168**, 715 (1970). Other references to Massachusetts Institute of Technology publications on frequency mixing and measurements of the speed of light are given here.
- C. Freed and A. Javan, *Appl. Phys. Lett.* **17**, 53 (1970).
- H. S. Boyne, J. L. Hall, R. L. Barger, P. L. Bender, J. Ward, J. Levine, J. Faller, in *Laser Applications in the Geosciences* (Western Periodicals, North Hollywood, California, 1970), p. 215; J. Levine, in *ibid.*, p. 227; J. Levine and J. L. Hall, *J. Geophys. Res.* **77**, 2595 (1972).
- M. S. Feld and A. Javan, *Phys. Rev.* **177**, 540 (1969); V. P. Chebotayev and I. M. Beterov, *Progress in Quantum Electronics* (Pergamon, New York, in press).
- H. R. Schlossberg and A. Javan, *Phys. Rev. Lett.* **17**, 1242 (1966).
- R. G. Brewer, *ibid.* **25**, 1639 (1970); in *Proceedings of the Esfahan Symposium on Fundamental and Applied Laser Physics* (Wiley, New York, in press).
- R. L. Shoemaker and R. G. Brewer, in preparation.
- A. C. Luntz, J. D. Swalen, R. G. Brewer, *Chem. Phys. Lett.* **14**, 512 (1972).
- See also A. C. Luntz, R. G. Brewer, K. L. Foster, J. D. Swalen, *Phys. Rev. Lett.* **23**, 951 (1969).
- A. C. Luntz, *Chem. Phys. Lett.* **11**, 186 (1971).
- S. H. Autler and C. H. Townes, *Phys. Rev.* **100**, 703 (1955).
- S. Haroche, C. Cohen-Tannoudji, C. Audoin, J. P. Schermann, *Phys. Rev. Lett.* **24**, 861 (1970).
- A. C. Luntz and R. G. Brewer, *J. Chem. Phys.* **53**, 3380 (1970).
- E. E. Uzgiris, J. L. Hall, R. L. Barger, *Phys. Rev. Lett.* **26**, 289 (1971).
- C. H. Anderson and N. F. Ramsey, *Phys. Rev.* **149**, 14 (1966).
- H. R. Schlossberg and A. Javan, *ibid.* **150**, 267 (1966).
- T. W. Hänsch, I. S. Shahin, A. L. Schawlow, *Phys. Rev. Lett.* **27**, 707 (1971).
- , *Nature* **235**, 63 (1972).
- G. W. Series, *Proceedings of the International Conference on Precision Measurements and Fundamental Constants*, G. N. Langenberg and B. N. Taylor, Eds. (National Bureau of Standards Special Publication 343, Government Printing Office, Washington, D.C., 1971), p. 73.
- R. G. Brewer and R. L. Shoemaker, *Phys. Rev. Lett.* **27**, 631 (1971).
- E. L. Hahn, *Phys. Rev.* **77**, 297 (1950).
- R. L. Shoemaker and R. G. Brewer, *ibid.*, in press.
- E. L. Hahn, *ibid.* **80**, 580 (1950).
- N. A. Kurnit, I. D. Abella, S. R. Hartmann, *Phys. Rev. Lett.* **13**, 567 (1964); *Phys. Rev.* **141**, 391 (1966).
- R. L. Shoemaker and R. G. Brewer, *Phys. Rev. Lett.* **28**, 1430 (1972).
- R. H. Dicke, *Phys. Rev.* **93**, 99 (1954).
- See E. D. Hinkley and P. L. Kelley, *Science* **171**, 635 (1971) for a review and references.
- O. G. Peterson, S. A. Tuccio, B. B. Snavely, *Appl. Phys. Lett.* **17**, 245 (1970).
- S. E. Harris, *Proc. IEEE* **57**, 2096 (1969).
- C. K. N. Patel and E. D. Shaw, *Phys. Rev. Lett.* **24**, 451 (1970).
- C. K. N. Patel, *ibid.* **28**, 649 (1972).
- A. Mooradian, S. R. J. Brueck, F. A. Blum, *Appl. Phys. Lett.* **17**, 481 (1970); S. R. J. Brueck and A. Mooradian, *ibid.* **18**, 229 (1971).
- T. Oka and T. Shimizu, *ibid.* **19**, 88 (1971).
- P. A. Steiner and W. Gordy, *J. Mol. Spectrosc.* **21**, 291 (1966).
- S. C. Wofsy, J. S. Muentzer, W. Klemperer, *J. Chem. Phys.* **55**, 2014 (1971).
- The author is indebted to E. K. Plyler for his unpublished spectrum of methane; to R. L. Shoemaker, E. L. Hahn, A. C. Luntz, and H. Morawitz for comments regarding this manuscript; and to K. Shimoda and T. Shimizu for their review manuscript prior to publication. Supported in part by ONR contract N00014-72-C-0153.

Particle Track Etching

Diverse technological uses range from virus identification to uranium exploration.

R. L. Fleischer, H. W. Alter, S. C. Furman,
P. B. Price, and R. M. Walker

In this article we describe a case in which the study of basic science has led to practical results—the case of particle track etching (1–4). We believe that the extreme versatility of this technique points out the essential unpredictability of the consequences of science and hence the opportunities inherent in understanding how things work.

In particular, we will describe here how the simple discovery of track etching has led to applications in semiconductor electronics, aerosol sampling, the identification of microbiological par-

ticles, nuclear engineering, mine safety, neutron radiography, uranium exploration, tracer technology, the determination of the color of gem diamonds, the clarification and stabilization of beer and wine, and a variety of peaceful uses for nuclear reactors. This list is but a sampling of a larger list, intended to convey the diversity of possibilities.

Observation of Particle Tracks

As a charged particle such as a fission fragment moves through a solid, it produces a region of permanent, catastrophic atomic damage (5). Examples of such damage tracks, first seen directly in transmission electron microscopy (6), are shown in Fig. 1A. The critical step that made it possible to use these tracks was the discovery that the damage could be preferentially dis-

Dr. Fleischer is with the General Electric Research and Development Center, Schenectady, New York 12301; Drs. Alter and Furman are with the General Electric Vallecitos Nuclear Center, Pleasanton, California 94566; Dr. Price is with the department of physics, University of California, Berkeley 94720; and Dr. Walker is with the department of physics, Washington University, St. Louis, Missouri 63130.